Supporting Information

Nitrogen-doped carbon nanotube encapsulated Fe$_7$S$_8$ nanoparticles for high-efficiency and selective removal of Pb^{2+} by pseudocapacitive coupling

Yong Gao,[a,†] Yingsheng Xu,[b,c,†] Shuhong Xiang,[b,c] Xinyuan Zhang,[b,c] Zhaolei Li,[a,*]

and Hongjian Zhou[b,c,*]

[a] *Department of Polymer Materials, School of Materials Science and Engineering, Jiangsu University of Science and Technology, Zhenjiang 212003, PR China*

[b] *Key Laboratory of Materials Physics, Centre for Environmental and Energy Nanomaterials, Anhui Key Laboratory of Nanomaterials and Nanotechnology, Institute of Solid State Physics, HFIPS, Chinese Academy of Sciences, Hefei, 230031 P. R. China*

[c] *Science Island Branch of Graduate School, University of Science and Technology of China, Hefei 230026, P. R. China*

[†] These authors contributed equally to this work.

* Email address: zlli@just.edu.cn (Z. Li) and hjzhou@issp.ac.cn (H. Zhou)

Experimental Section

Materials. The commercial melamine foam was obtained from Puyang Lvyu Foam Co., Ltd. Iron(III) nitrate nonahydrate ($Fe(NO_3)_3 \cdot 9H_2O$) and urea were bought from Aladdin. Sulfur powder, lead nitrate, sodium chloride and thiourea were bought from Sinopharm Chemicals, China. Activated carbon was bought from Fuzhou Yihuan Carbon Co., Ltd., China. Poly(vinylidene fluoride) (PVDF) was received from Tianjin Aiweixin Chemical Technology Co., Ltd. Ketjen black was purchased from Suzhou Yilongsheng Energy Technology Co., Ltd. All purchased reagents were analytically pure without further treatment.

Materials characterization. The surface morphology of the prepared samples was determined by the SEM (SU 8020) and HRTEM (JEOL-2010) equipped with an energy-dispersive spectrometer (EDS, OXFORD). Using X-ray diffractions (XRD, X'Pert, Netherlands) and Raman spectra (Confocal microscope Raman Spectroscopy, Renishaw inVia Reflex, Britain) to characterize the structures of the materials above. The specific surface area and pore size distribution were measured by nitrogen adsorption-desorption isotherm on an automatic gas adsorption analyzer (Autosorb-iQ-Cx) according to the Brunauer-Emmetl-Teller (BET) and Barrett-Joyner-Halenda (BJH) methods, respectively. X-ray photoelectron spectroscopy (XPS) analysis was performed on an ESCALAB 250 X-ray photoelectron spectrometer (Thermo, America) equipped with Al Kα1, 2 monochromatized radiations at 1486.6 eV X-ray source.

Electrochemical characterization of Fe_7S_8@NCNT. The electrochemical performance of the Fe_7S_8@NCNT was measured with an electrochemical workstation (CHI 660E, CH Instrument, Inc., shanghai, China) in 1.0 M NaCl solution, including cyclic voltammetry (CV), galvanostatic charge/discharge (GCD), electrochemical impedance spectroscopy (EIS). To prepare the working electrodes, active substance (Fe_7S_8@NCNT), Ketjen black (ECP60JD) and poly vinylidene fluoride (PVDF, Solef 5130) were mixed at a mass ratio of 8:1:1 in N-Methyl pyrrolidone (NMP) solution to

form a homogeneous slurry. The mixture was coated onto the Ni foam substrate, and then dried at 70 °C for 12 h. The Ag/AgCl and Pt as reference electrode and counter electrode, respectively. The CV measurements were carried out at different scanning rates from 3 to 50 mV s^{-1} in the potential range of -0.2~-1.0 V. The GCD was performed at various current densities from 0.5 to 20 A g^{-1} in the potential range of -0.2~-1.0 V. The EIS was conducted with an amplitude of 5.0 mV and frequency range from 0.01 Hz to 1 MHz.

DFT calculations. All DFT calculations were simulated with the software of Materials studio 2018. Given the experimental XRD results, the crystal model of Fe_7S_8 was built according to previous reports [1, 2]. All model structures were further optimized by CASTEP package. During the structure optimization process, generalized gradient approximation (GGA) with function of Perdew-Burke-Ernzerhof (PBE) was employed to describe the electron interaction energy of exchange correlation. In the calculation of partial density of state (PDOS) toward the three crystals, the energy convergence tolerance of 2.0×10^{-6} eV atom^{-1}, energy cutoff of 330 eV, and pseudopotentials of ultrasoft were applied. During adsorption calculation, cleaving adsorption surface was based on strongest diffraction peak of (2 0 6) plane and 10 Å vacuum layers was built to prevent interactions between the two repeated layers. The adsorption energy (ΔE_a) of cations were calculated by following equation:

$$\Delta E_a = E_{Fe_7S_8 + cation} - E_{Fe_7S_8} - E_{cation} \qquad (S1)$$

where E (eV) indicates the final energy of models after structure optimization.

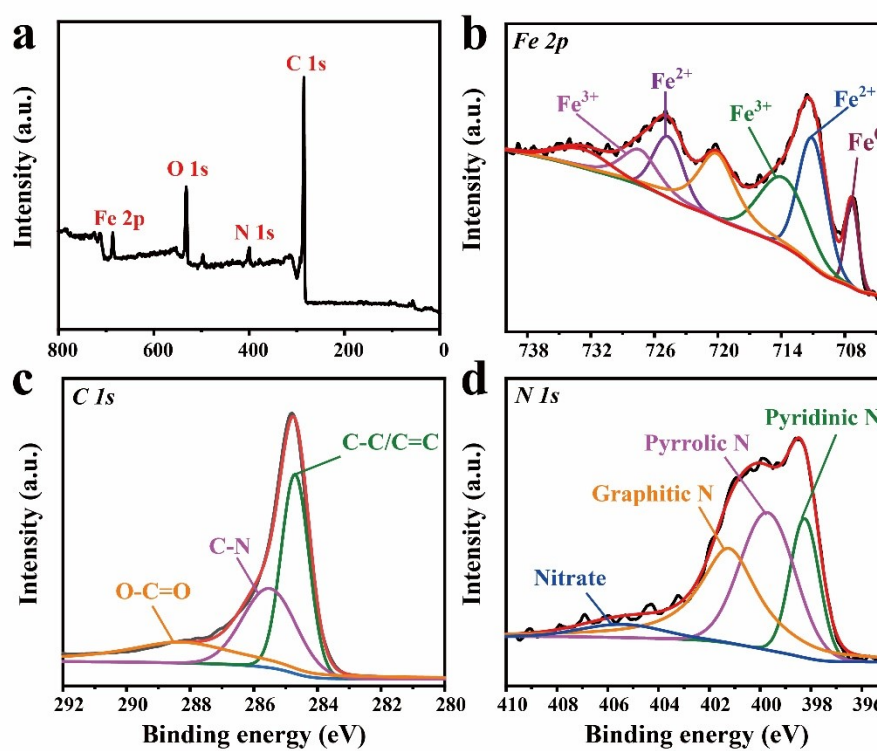**Fig. S1**. Photograph of home-made real-time current and energy consumption detector.

Fig. S2. (a) XPS survey of $Fe_3C/NCNT$; (b) Fe 2p, (c) C 1s and (d) N 1s XPS spectra of $Fe_3C/NCNT$.
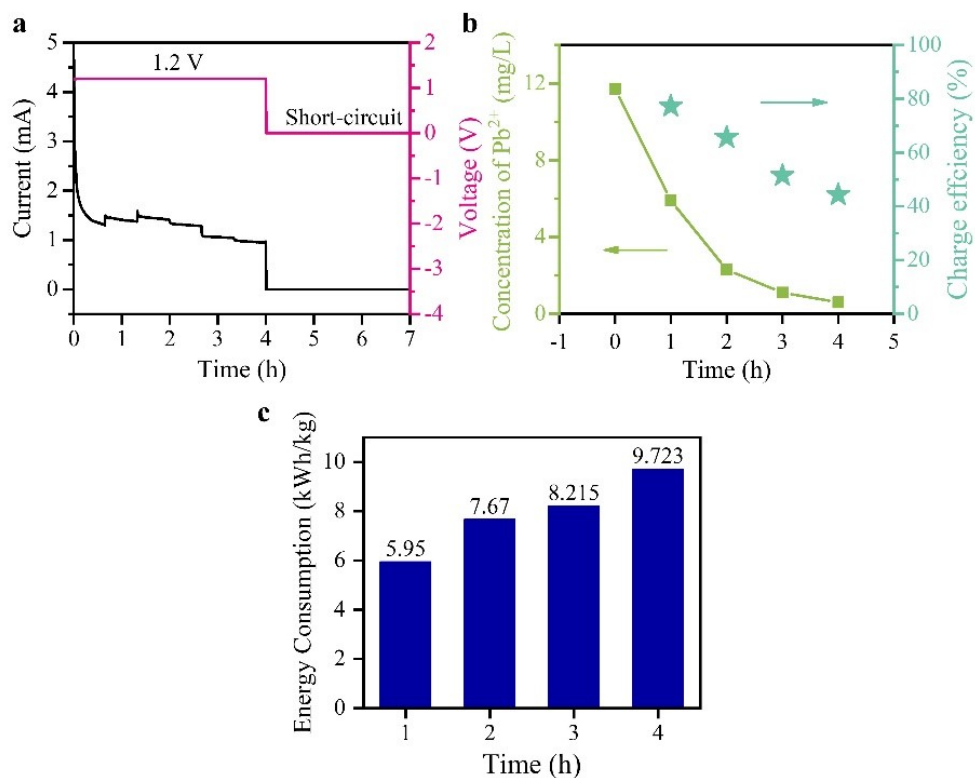
Fig. S3. (a) Time-dependent current curve during electrosorption (1.2 V) and desorption; (b) Concentration variation of Pb^{2+} ion during electrosorption and corresponding calculated charge efficiency; (c) Energy consumption during electrosorption process.
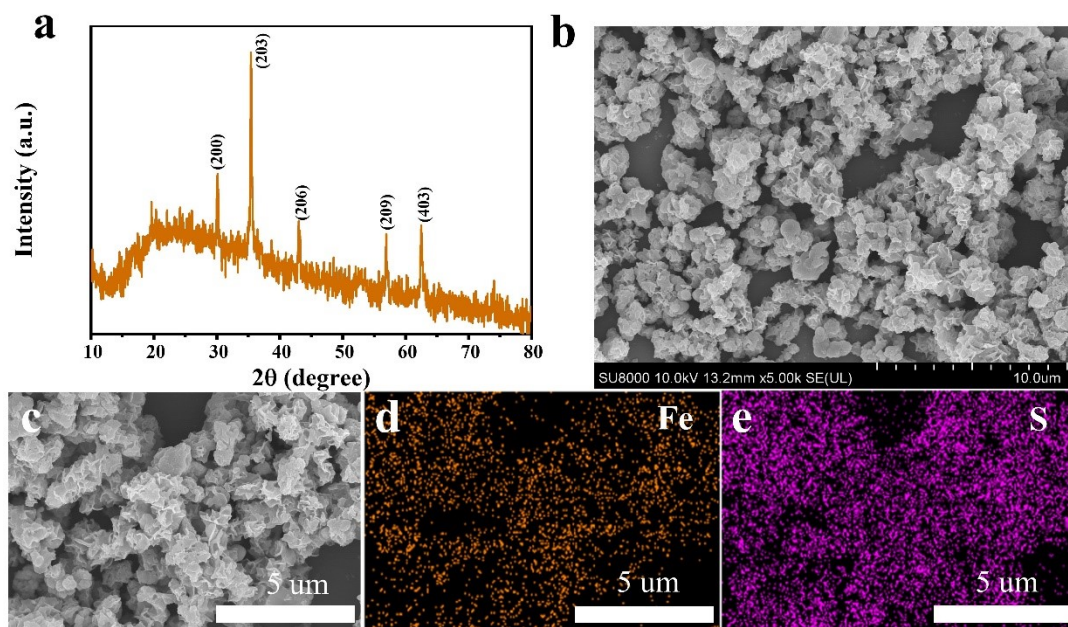

Fig. S4. (a) XRD and (b) morphology of of as-prepared Fe_7S_8 nanoflower by one-step hydrothermal; (c), (d) and (e) corresponding EDS mapping images.
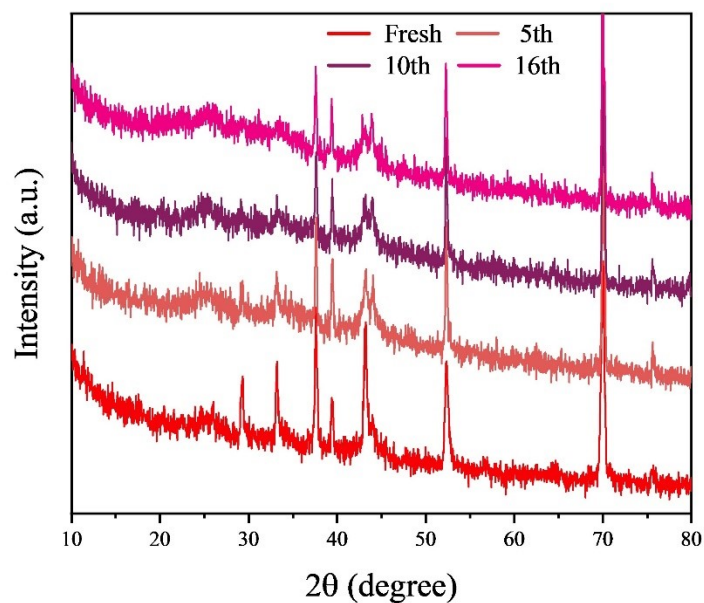
Fig. S5. (a) XRD spectra of fresh or desorbed Fe_7S_8@NCNT electrode at various cycled periods.

Table S1. Specific surface area (SSA) and pore volume (V_{pore}) of different samples.

Element	SSA ($m^2 g^{-1}$)	V_{pore} ($cm^3 g^{-1}$)
Fe_3C@NCNT	181.2	0.41
Fe_7S_8@NCNT	26.8	0.076

Table S2. The calculated value of R_s and R_{ct} fitted from EIS curves according to the equivalent circuit.

Samples	R_s (Ω)	R_{ct} (Ω)
Fe_3C@NCNT	3.71	0.113
Fe_7S_8@NCNT	3.31	0.014

References

1. H. Kobayashi, M. Sato, T. Kamimura, M. Sakai, H. Onodera, N. Kuroda and Y. Yamaguchi, *J. Phys.: Condens. Matter.*, 1997, **9**, 515-527.

2. F. Kellerbesrest, G. Collin and R. Comes, *Acta Crystallogr., Sect. B: Struct. Sci.*, 1983, **39**, 296-303.